



**HAL**  
open science

## Human serum albumin nanoparticles as nanovector carriers for proteins: Application to the antibacterial proteins “neutrophil elastase” and “secretory leukocyte protease inhibitor”

Mohamad Tarhini, Anne Pizzoccaro, Ihsane Benlyamani, Chloé Rebaud, Hélène Greige-Gerges, Hatem Fessi, Abdelhamid Elaïssari, Abderrazzak Bentaher

### ► To cite this version:

Mohamad Tarhini, Anne Pizzoccaro, Ihsane Benlyamani, Chloé Rebaud, Hélène Greige-Gerges, et al.. Human serum albumin nanoparticles as nanovector carriers for proteins: Application to the antibacterial proteins “neutrophil elastase” and “secretory leukocyte protease inhibitor”. *International Journal of Pharmaceutics*, 2020, 579, pp.119150. 10.1016/j.ijpharm.2020.119150 . hal-02988947

**HAL Id: hal-02988947**

**<https://hal.science/hal-02988947>**

Submitted on 22 Aug 2022

**HAL** is a multi-disciplinary open access archive for the deposit and dissemination of scientific research documents, whether they are published or not. The documents may come from teaching and research institutions in France or abroad, or from public or private research centers.

L'archive ouverte pluridisciplinaire **HAL**, est destinée au dépôt et à la diffusion de documents scientifiques de niveau recherche, publiés ou non, émanant des établissements d'enseignement et de recherche français ou étrangers, des laboratoires publics ou privés.



Distributed under a Creative Commons Attribution - NonCommercial 4.0 International License

## Title

### Human serum albumin nanoparticles as nanovector carriers for proteins: Application to the antibacterial proteins "neutrophil elastase" and "secretory leukocyte protease"

Mohamad Tarhini<sup>a,b</sup>, Anne Pizzoccaro<sup>c</sup>, Ihsane Benlyamani<sup>a</sup>, Chloé Rebaud<sup>c</sup>, H el ene Greige-Gerges<sup>b</sup>, Hatem Fessi<sup>a</sup>, Abdelhamid Elaissari<sup>a\*</sup>, Abderrazzak Bentaher<sup>c</sup>

<sup>a)</sup> Univ Lyon, University Claude Bernard Lyon-1, CNRS, LAGEP UMR 5007, 43 boulevard du 11 November 1918, F-69100, Villeurbanne, France

<sup>b)</sup> Faculty of Sciences, Lebanese University, B.P. 90656, Jdaidet El-Matn, Lebanon

<sup>c)</sup> Inflammation and Immunity of the Respiratory Epithelium - EA 7426, Faculty de Medicine Lyon Sud, 69495, Pierre Benite, France

Correspondence: [abdelhamid.elaissari@univ-lyon1.fr](mailto:abdelhamid.elaissari@univ-lyon1.fr)

#### Abstract

The use of proteins and defined amino acid sequences as therapeutic drugs have gained a certain interest in the past decade. However, protein encapsulation within protein nanoparticles was never endeavored. For this reason, human serum albumin (HSA) nanoparticles were prepared by nanoprecipitation method. The process was optimized, and particles were obtained with a size of 120 nm and zeta potential of -25 mV. Neutrophil elastase (NE) and secretory leukocyte protease inhibitor (SLPI) were encapsulated separately within HSA nanoparticles. Gel electrophoresis and western blot studies demonstrate the successful encapsulation and the stability of the particles. On the other hand, enzymatic assays show that encapsulated NE lost its proteolytic activity, whereas encapsulated SLPI maintained its inhibitory property. In addition, the antibacterial studies showed that both formulations were able to drastically reduce bacterial growth of *Pseudomonas aeruginosa*. This work showed the possibility of using both NE and SLPI as anti-bacterial agents through encapsulation within HSA nanoparticles.

**Keywords:** protein nanoparticles ; elastase ; enzyme encapsulation ; antibacterial ; SLPI

## 1. Introduction

Protein based nanoparticles are gaining some attention as drug vehicles. Their magnitude results from their unique features among other nanoparticles building materials. They hold biocompatibility, bio functionality, and safe biodegradability into amino acids (Tarhini et al., 2017). A variety of proteins were previously used as building blocks for nanocarriers for small molecules. Gelatin, albumin, gliadin, zein, and other proteins were successfully used for cancer therapy and for carrying small molecules through the blood brain barrier (Elzoghby et al., 2015, 2012). Probably the most interesting protein to be discussed is human serum albumin (HSA). HSA is the most abundant plasma protein; it has a molecular weight of 66 kDa. Its main role is to preserve the colloidal osmotic pressure of the blood. Besides, it acts as a transporter vehicle of metals and ions in the blood, it binds a tremendous number of therapeutic drugs, and when it degrades into amino acid, it can provide nutrition to peripheral tissues (Kratz, 2008). Actually, Abraxane<sup>®</sup>, a HSA nanoparticle formulation loaded with paclitaxel, was approved by the FDA for a variety of cancers (Zhao et al., 2010). Many preparation methods were used to formulate HSA nanoparticles such as emulsification, nanoparticle albumin bound technology, spray drying, and others (Tarhini et al., 2017). However, research lacks any attempt of HSA nanoparticle synthesis through nanoprecipitation. This method is composed of only one step, fast and easy to reproduce, and usually do not require any shear force that can lead to disruption of macromolecules. Yet, it was always known for the preparation of nanoparticles from hydrophobic materials. In addition to that, literature lacks any attempt of encapsulating protein molecules within protein nanostructure. Theoretically, such a system can benefit from the similarity between the carrier and the drug since both are made from amino acids. Plus, this protein-crowded environment can mimic the protein-inhabited environment in the body (Herrera Estrada and Champion, 2015).

Human neutrophil elastase (NE) is a serine protease of the chymotrypsin family, produced by neutrophils and plays an important role in the elimination of the extracellular pathogens and breaking down host tissue at inflamed sites. It has a molecular weight of 34 kDa. This enzyme has been reported to play a relatively important role in neutrophil-mediated bacterial killing. It was found that NE-deficient mice were more susceptible to Gram-negative bacteria-mediated sepsis and death than their wild type littermates. Paradoxically, it has been shown that unchecked NE could participate in the pathogenesis of neutrophil-rich lung inflammatory and tissue destructive diseases. This protease was reported to cleave E-cadherin in both cell culture system and a mouse model of acute lung injury. Taken into consideration NE biologic properties, its use as a therapeutic anti-bacterial agent would require an approach that prevents its deleterious effect of host tissue-degrading protease. This can be theoretically achieved by encapsulating NE within a drug carrier. A nanoparticle formulation might indeed reduce NE host injuring effects while ensuring its protection from host-derived inactivation (e.g., oxidants and physiologic inhibitors) (Lerman and Hammes, 2018; Tsai and Hwang, 2015)

Secretory leukocyte protease inhibitor (SLPI) is a 12 kDa protein produced by cells of human airways mucosa and can be found in all body fluids such as salivary glands, tears, bronchial secretions, seminal fluids, and intestinal mucus. SLPI is known to inhibit NE and prevents its proteolytic enzyme that can cause epithelial injury if unchecked. In addition, it has an anti-microbial role where its activity against *Escherichia coli*, *Pseudomonas aeruginosa*, *Staphylococcus aureus*, *Staphylococcus epidermidis*, and human immunodeficiency virus (HIV) has been reported (Majchrzak-Gorecka et al., 2016).

In this work, NE and SLPI were encapsulated within HSA based nanoparticles, NE-HSA-NPs and SLPI-HSA-NPs respectively. The effect of various experimental parameters on the preparation of such particles was investigated, and the colloidal properties of the obtained dispersions were examined. In addition, special attention has been dedicated to the antibacterial activity of the formulated dispersions. The inhibitory activity of SLPI against neutrophil elastase was also studied.

## **2. Materials and Methods**

### **2.1. Materials**

Human serum albumin (HAS), dimethyl sulfoxide (DMSO), and sodium hydroxide were purchased from Sigma-Aldrich. Glutaraldehyde solution 25%, ethanol 96% and hydrogen chloride were provided by VWR BDH prolabo (France). Sodium chloride, disodium phosphate, and monosodium phosphate were provided by Merck GmbH (France). Electrophoresis gel components: acrylamide 40%, Tris electrophoresis purity reagent, sodium dodecyl sulfate, ammonium persulfate, and TEMED were all provided by Biorad. NE and SLPI were purchased from Sigma-Aldrich and abcam (France).

### **2.2. Preparation and optimization of blank HSA-NPs**

HSA-NPs were prepared by nanoprecipitation method first developed by Fessi et al. (Fessi et al., 1989). In brief, a given amount of HSA was dissolved in water. Under magnetic stirring of 300 rpm, a non-solvent phase consisting of ethanol was added to the HSA aqueous phase. The mixture became instantaneously milky-like indicating the construction of the particles. After that, 10  $\mu$ l of glutaraldehyde 25% was added to the mixture and kept under stirring overnight. Ethanol was then removed by rotary evaporation at 30 °C and 100 rpm using BUTCHI rotavapor® R-100.

### **2.3. Preparation of NE-HSA-NPs, and SLPI-HSA-NPs**

HSA 2% (w/v) aqueous solution was prepared by dissolving 0.1 g of HSA in 5 ml water. NE (100  $\mu$ l at 0.5  $\mu$ g/ $\mu$ l) was added to the solution under magnetic stirring to obtain NE-loaded HSA nanoparticles (NE-HSANPs). SLPI (100  $\mu$ l of SLPI at 1.5  $\mu$ g/ $\mu$ l) was added to obtain SLPI-loaded HSA nanoparticles (SLPI-HSA-NPs). Then, ethanol was added with a water/ethanol ratio of 1/2 and kept under stirring at low temperature. The mixture was removed and lyophilized for 72 hours using Cryonext Lyophilisator with a maximum temperature limit of 4°C. Particles were then re-dispersed in DPB (+) solution and stored at -20 °C until use. In both cases, during the preparation, temperature was kept low by using cold solvents and the precipitation was done in an ice bath.

### **2.4. Characterization of nanoparticles**

Loaded and blank HSA nanoparticle dispersions were characterized in terms of size, distribution, and electrokinetic properties. Size and zeta potential were measured using a Malvern Zetasizer (model nano ZS) by photon correlation spectroscopy and electrophoretic mobility measurement respectively. Size was calculated by means of the Stokes-Einstein equation from the diffusion coefficient measured by dynamic light scattering (39). Zeta potential was deduced from the measured electrophoretic mobility using the Helmholtz–Smoluchowski equation.

### **2.5. Gel electrophoresis**

All samples were migrated under non-reducing conditions on SDS-PAGE gels (10%). Following electrophoresis, gels were stained in Coomassie blue reagent and de-stained in 5% acetic acid and 10% methanol. Gel visualization and images acquisition were performed using ChemiDoc XRS (Bio-Rad).

## 2.6. Western blot

NE loaded samples were separated on 10% SDS-PAGE gels and transferred to nitrocellulose membranes (Hybond ECL, Amersham Pharmacia Biotech., Buckinghamshire, UK) in 48 mM Tris, 30 mM glycine, 20% methanol, and 0.0375% SDS. Non-specific binding sites were blocked by soaking the membranes in 3% non-fat dry milk in Tris-buffered saline at 4° C overnight. Blots were incubated with a 1:500 dilution of anti-NE polyclonal antiserum (1:500), anti-SLPI polyclonal antiserum (1:200), or anti-HSA polyclonal antiserum (1:500) in blocking buffer for 1 h and washed twice with Tris-buffered saline containing 0.1% Tween-20 for 10 min. Membranes were subsequently incubated with an appropriate dilution of peroxide-linked secondary IgG in blocking buffer for 1 h, washed twice and developed with ECL system according to the manufacturer's instructions. Images were acquired using ChemiDoc XRS (Bio-Rad).

## 2.7. Enzymatic activity

The inhibitory activity of SLPI against neutrophil elastase was tested. In a 96-well microtiter format, free SLPI, dissolved HSA, blank HSA nanoparticles, and SLPI loaded HSA nanoparticles were introduced in the presence of NE (6.6nM) in buffer (0.05M Hepes buffer, 0.1M NaCl, 0.05% NP40, pH 7,5) using 500 $\mu$ M N-methoxy succinyl-Al-Al-Pro-Val-pNA (MeOSuc-AAPV-pNA) as chromogenic substrate. The activity of NE was monitored spectrophotometrically at 410nm in the reader chamber of a multiskan Ascent plate reader every 10 s for 15 minutes. The activity of free SLPI was tested against NE and different SLPI concentrations (1 mM, 100  $\mu$ M, and 10  $\mu$ M), while for the particles and dissolved HSA, it was evaluated at the following concentrations (20  $\mu$ g/ $\mu$ l, 0.31  $\mu$ g/ $\mu$ l, 0.15  $\mu$ g/ $\mu$ l, 0.06  $\mu$ g/ $\mu$ l, and 0.03  $\mu$ g/ $\mu$ l). A total volume of 150  $\mu$ l of incubation mixture was used for each well and the enzymatic assays were initiated by the addition of the substrate. Each measurement was repeated at least three times to achieve reproducibility. A positive control containing NE (6.6nM) in buffer (0.05M Hepes buffer, 0.1M NaCl, 0.05% NP40, pH 7,5) were run under the same conditions. In addition, the enzymatic activity of encapsulated NE (NE-HSA-NPs) was also evaluated. Illustration on the preparation method is present in the results parts in **figure 4**.

## 2.8. Antibacterial activity assay

The antibacterial activity of filter-sterilized NE, SLPI, NE-HSA-NPs, and SLPI-HSA-NPs was investigated against *Pseudomonas aeruginosa* H103 bacteria (41). Overnight cultures of bacteria were diluted in half and grown aerobically in Luria Bertani broth (10 ml) at 37°C to late exponential phase (3 h). Bacteria were collected by centrifugation (500g, 10 min), washed twice, and resuspended in 1 ml of PBS (pH 7.4). Bacterial turbidity was determined from the optical density at 600 nm wavelength (OD 10<sup>7</sup> 10<sup>9</sup> bacteria/ml). Bacteria (10<sup>7</sup>) were then added to NE, SLPI or NE- or SLPI-loaded HSA particles in a total volume of 200  $\mu$ l and incubated for three hours at 37°C under gentle shaking. Next, serial dilutions were spread on agar plates and the number of CFUs was determined after overnight incubation.

## 2.9. Statistical analysis

Statistical analyses were performed using Student's t test and ANOVA. Significance was accepted at  $p < 0.05$ . Results are expressed as mean  $\pm$  SEM.

## 3. Results and discussion

### 3.1. Effect of nanoprecipitation parameters on the colloidal properties of HSA-NPs

HSA-NPs were prepared by nanoprecipitation method, and the effect of HSA concentration, solvent/non-solvent volume ration (S/NS), ethanol addition speed, ionic strength, and pH on the size

and zeta potential was evaluated to deduce the optimal preparation conditions (**Figure 1**). It must be emphasized that all characterized dispersions have been performed after solvent removal.

First, particles were prepared with a different initial amount of HSA (from 1% to 3% w/v) and S/NS ratio of 1:2 (**Figure 1.A**). no significant change was observed in size and zeta potential of the particles. The chosen concentration has no effect on the colloidal properties of the particles. However, the polydispersity index (PDI) values. This observation is in good agreement with the work reported by Langer et al. where HSA-NPs prepared by desolvation method, shows no significant variation on the hydrodynamic size when the HSA amount is ranging between 2.5 and 10% (w/v) (Langer et al., 2003). The same behavior can be observed with zeta potential. However, the polydispersity index achieves a minimum with 2% initial concentration (PDI = 0.02) indicating that samples are more narrowly size distributed. Monodispersity is an important factor in pharmaceutical formulations, since it can give higher reproducibility of the samples, good colloidal stability of the particles, and better homogeneity of active ingredient in later dosage form (Danaei et al., 2018). Therefore, HSA initial amount of 2% was selected to be used for the rest of optimization studies.

In addition, the effect of S/NS ratio on hydrodynamic size and the zeta potential of the obtained nanoparticles has been investigated and the obtained results are reported in **Figure 1.B**. It was found that the average hydrodynamic size of nanoparticles increases slightly with increasing the S: NS volume ratio until reaching maximum size for S: NS= 1:2 (before continuous decrease with increasing S/NS). The increase in size can be attributed to changes in the conductivity of ethanol water mixture step of nanoprecipitation. As mentioned above, by increasing the amount of ethanol over water (**left part in Fig. 1.B**), the quality of solvent medium diminishes for HSA, which induces protein precipitation. This may lead to more nuclei on one hand and large particle size on the other hand (if we assume that, the precipitation of proteins is a continuous process on rapid preformed nuclei). It is interesting to mention here, that in this first part of the graph, all proteins did not precipitate at low ethanol volume. In the vicinity of S: NS=1:2, the hydrodynamic size and zeta potential are found to be almost constant. This could be attributed to the complete precipitation of all proteins under nanoparticles form. By increasing ethanol (i.e. S: NS less than 1:2), this can induce more compact particles rather than the formation of more nuclei and consequently leading to increasingly small hydrodynamic size. By lowering ethanol volume, the supersaturation rate became lower and lead to larger nanoparticles (Joye and McClements, 2013). However, the decrease in size when lowering S: NS from 1:2 to 1:1 can be attributed to non-sufficient condition for successfully starting nanoprecipitation process. This can explain the large increase in PDI when S: NS is 1:1.

The obtained zeta potential values also show dependence to the S: NS used. From S: NS 1:3 to 1:2, the zeta potential value of the nanoparticles decreases from -17 to -25 mV. Then zeta potential increases from -25 to -17 when changing S: NS from 1:2 to 1:1 (**Figure 1.B**). As a general tendency, the observed zeta potential in absolute values are higher than 15 reflecting the good colloidal stability of the formulated dispersions due the strong electrostatic repulsion between the particles (Haro-Pérez et al., 2003).

*Figure 1: size, zeta potential, and PDI of HSA nanoparticles prepared by nanoprecipitation method with the variation of the following parameters. A) HSA% (w/v); B) Solvent: non-solvent volume ratio; C) ethanol addition speed in ml/h; D) phosphate buffer concentration in mM; and E) pH. F) size distribution of HSA nanoparticle formulation measured by DLS and made with the following parameters: 2% HSA; S: NS = 1:2; batch addition of ethanol; un-adjusted pH (around 6.7).*

The addition speed of ethanol was controlled using a syringe pump, and the effect of the speed is shown in **figure 1.C**. At 6 ml/h, high polydispersity index (PDI) can be observed (0.8) and decrease to 0.2 while increasing the speed to 120 ml/h. However, between 15 and 120 ml/h, particles maintain their hydrodynamic size (around 450 nm). This indicates that the higher the addition rate of the non-solvent, the better the precipitation process. Probably caused by more overwhelming supersaturation. Zeta potential also decreases from -25 to -23 mV while increasing the speed from 5 to 120 ml/h. Still, a better size/charge/distribution profile can be achieved with a batch addition of ethanol to induce precipitation.

HSA nanoparticles were prepared at different phosphate buffer concentrations (**Figure 1.D**). It was learnt that an increase in phosphate buffer concentration in the nanoprecipitation formulation leads to an increase in hydrodynamic size of the particles. As expected, the increase in ionic strength reduces the repulsive electrostatic interaction between protein molecules, consequently, increasing the size of the resulting particles. It's interesting to note, that high salinity was generally used to induce precipitation of proteins before purification and analysis step. The non-aggregation of the obtained nanoparticles at moderate salinity (10, 20, and 30 mM) can be attributed to repulsive hydration forces between particles and also to repulsive electrostatic interactions. However, the large size observed at high phosphate buffer concentration can be attributed to nanoparticles aggregation during the formation process. Regarding the electrokinetic property of the prepared particles in function of buffer concentration. The zeta potential was found to decrease (in absolute value) with increasing the buffer concentration. This can be attributed to the screening of the surface charge density, which affects the average shear plane position by shifting this close to the surface (Chaix et al., 2003). Consequently, the zeta potential decreases in absolute value.

Finally, the pH adjustment has a marked influence on the size and zeta potential of HSA-NPs (**Figure 1.E**). By increasing the pH from 2 to 11, the size decreases from 330 to 90 nm. In addition, the zeta potential also decreases from 25 mV to -25 mV. HSA is a negatively charged protein with an isoelectric pH of 4.7. It is known that below the isoelectric point of protein, most of the carboxyl and amino groups are protonated leading to a net positive charge. Above the isoelectric point, these groups are non-protonated and so the net charge is negative. This explains the shifting in the zeta potential value from 25 to -25 mV. As for the size decrease, the same effect of ionic strength increase can be applied to pH variation. These differences in charges can cause variation in the electrostatic repulsion of protein and induce aggregation translated with bigger sized particles (Davidov-Pardo et al., 2015).

These findings show the possibility of controlling the colloidal properties of HSA nanoparticles by varying the experimental parameters of the nanoprecipitation process. Additionally, the limits of some parameters were also found. This will allow us to choose the desired formulation for future studies. Ideally, the desired formulation is to have the smallest size and highest absolute value of zeta potential with the lowest polydispersity. This can be achieved either in buffered or un-buffered conditions. But for the sake of simplicity, the optimal formulation was prepared in water, with 2% HSA initial concentration, S: NS of 1:2, and with a batch addition of non-solvent. **Figure 1.F** represents the size distribution of this formulation.

### **3.2. Characterization of NE-HSA-NPs and SLPI-HSA-NPs**

The entrapment of NE and SLPI separately within HSA nanoparticles has an effect on their properties (**Figure 2.A**). In both cases, a small increase in size was observed depending on the size of the enzymes themselves. NE-HSA-NPs have a size of 150 nm and SLPI-HSA-NPs have a size of 127 nm. While HSA-NPs are 120 nm in size. A narrow size distribution is observed for all the three formulations (**Figure 2.B**). However, it can be observed that the dispersity of the particles increases after loading with both NE and

SLPI. This can be attributed to the non-uniform distribution of the drug within the particles. Since the chosen process was not optimized to obtain uniformly distributed encapsulated drug. This increase in size is accompanied with a decrease in charge of the particles. Both NE and SLPI-HSA-NPs have a lower negative charge than the blank particles. This decrease in charge is caused by the positive charge of NE and SLPI. The encapsulation was done in a pH of approximately 6.7, this value is below the isoelectric point (IEP) of NE and SLPI and above the IEP of HSA. For this reason, blank HSA particles are more negative than the loaded one. In addition, this suggests that the interaction between HSA and NE/SLPI is mainly electrostatic in nature. Furthermore, this finding can point towards the position of NE and SLPI within the protein matrix. The decrease in surface charge for the loaded formulation indicates that the positively charged NE and SLPI reside on the surface of the HSA nanoparticles.

*Figure 2: HSA-NPs, NE-HSA-NPs, and SLPI-HSA-NPs: A) Size, zeta potential, and PDI; B) size distribution by DLS*

### 3.3. Gel electrophoresis and western blot

Gel electrophoresis has been used to investigate the composition of the formulated dispersions. Even for nanoparticles composed from no biological materials such as gold and silver nanoparticles, they can be separated by coating them with a polymer layer and the separation can be done according to size, shape or surface charge of the nanoparticles (Hanauer et al., 2007). Moreover, bovine serum albumin (BSA) based nanoparticles were previously migrated in an SDS-polyacrylamide gel at different concentrations next to dissolved BSA solution to investigate the purity of the particles. It was found that the protein bands and the nanoparticles bands clearly demonstrates a high purity of the product (Rahimnejad et al., 2006). In other study, the packaging of a plasmid within HSA-polyethyleneimine nanoparticles was also investigated by gel electrophoresis (Rhaese et al., 2003). In this study, HSA-NPs, NE-HSA-NPs, and SLPI-HSA-NPs were migrated at increased concentration (**Figure 3.A-C**). HSA-NPs were migrated at increased concentrations (0.5, 1, 2.5 and 5  $\mu$ g) (**Figure 3.A**), and Coomassie staining showed increased staining intensity but a single band in all lanes indicating the absence of degradation in HSA molecules. Likewise, NE-HAS-NPs and SLPI-HSA-NPs Coomassie staining also showed a single band (around 66 kDa) in all lane with an increasing intensity (**Figure 3.B and C**). The absence of a separate band for NE and SLPI in **Figure 3.B** and **figure 3.C** respectively can indicate two possibilities. Either NE and SLPI are completely complexed with the HSA matrix within the nanoparticles, or the amount of NE and SLPI are below the detection limit. To answer this, another migration was performed for HSA-NPs, NE-HSA-NPs, NE in the presence of free HSA molecules (HSA + NE), and HSA in non-particulate form (**Figure 3.D**). HSA-NPs and NE-HSA-NPs have the same band of the previous results, however, when we introduced NE and HSA separately (NE + HSA), we were able to observe a separate band for NE at about 34 kDa corresponding to its molecular weight. In this migration, the amount of NE used was similar to the lowest concentration introduced in **figure 3.B**. From this observation we were able to dismiss the possibility of a low detection limit while confirming the entrapment of NE molecules within the HSA matrix. The same study was performed with SLPI and similar results were obtained (data not shown).

*Figure 3: Protein gel electrophoresis at different concentrations of A) HSA-NPs B) NE-HSA-NPs; C) SLPI-HSA-NPs. D) Protein gel electrophoresis of HSA-NPs, NE-HSA-NPs, free HSA and free NE and free HSA alone. Western blot micrographs of E) NE-HSA-NPs and F) SLPI-HSA-NPs.*

To our knowledge, there is no reported studies on the interaction between HSA and NE or HAS and SLPI molecules. However, the binding between NE and albumin (BSA) was investigated briefly by Biaci et al. In their work, they use bovine serum albumin as a protein model, it was found that albumin can rapidly form a reversible complex with NE that can be dissociated in the presence of other factors such as eglin



C (Baici, 1990). In addition, the isoelectrical point (IEP) of HSA and NE are 4.7 and 8.65 respectively, and the pH during the precipitation was about 6.5. This will induce a negative charge to HSA and a positive charge to NE which increase the likelihood of electrostatic interaction between HSA and NE (Kratz, 2008; Miller et al., 1989).

To establish that the performed encapsulation method is successful, we carried out immunoblotting experiments using antibodies specific to HSA, NE and SLPI. The samples were run as described above and the gels were processed for immunodetection of HSA, NE and SLPI. The obtained results show specific immunostaining for HSA (data not shown), SLPI and NE (**Figure 9.E and F**). This migration confirms the association between HSA and NE or SLPI molecules and strongly suggest that the encapsulated forms contain both HSA and NE or SLPI in the form of NE-HSA-NPs and SLPI-HSA-NPs respectively.

### 3.4. Enzymatic activity assay

The activity of elastase was evaluated in the presence of dissolved HSA, HSA-NPs, SLPI-HSA-NE, and when NE was in an encapsulated form NE-HSA-NPs (**Figure 4**). It was found that in the presence of dissolved HSA, the activity of NE increases with increasing HSA concentration. The lowest activity was recorded in the absence of HSA in the medium (**Figure 4.A**). In a study performed on the *in vitro* inhibition of NE, the inhibition of NE by colistin and tobramycin was reduced in the presence of albumin and the activity of elastase in the presence of albumin increase significantly (Hector et al., 2010). In another study, albumin with a range between 0.1 – 0.3 g/L was able to increase the activity of elastase 3-fold (Edwards et al., 2004).

*Figure 4: Enzymatic activity of NE against its chromogenic substrate. A) in the presence of dissolved HSA molecules, B) in the presence of HSA-NPs, C) NE entrapped within NE-HSA-NPs, and D) in the presence of SLPI-HSA-NPs.*

In the presence of HSA-NPs (**Figure 4.B**), the opposite can be observed. Blank nanoparticles were able to intensely reduce the activity of the enzyme irrespective of HSA concentration. This observation can be attributed to electrostatic interactions between NE molecules and HSA-NPs. NE molecules that are bound to the nanoparticles would not engage in the proteolytic activity against the chromogenic substrate. This will hinder the enzymes turnover of available substrate, thereby decreasing the initial velocity of elastase hydrolysis. However, an increase in absorbance can be observed between 0 and 900 seconds indicating the presence of NE activity that can be attributed to free NE molecules.

Another assay was performed for nanoparticles loaded with NE (**Figure 4.C**). In this study, the absorbance was found to be stable during as a function of time of measurement. Indicating that NE was indeed entrapped within NE-HSA-NPs and was not released during the selected experimental condition. From these results, it can be deduced that the encapsulation of NE may affect its *in vitro* proteolytic activity. This is particularly interesting as NE loaded formulation can be used as anti-bacterial agents without inducing proteolytic side effects.

Finally, the inhibition of NE activity by SLPI-HSA-NPs was evaluated (**Figure 4.D**) and it was found that these formulations eliminate the activity of the enzyme. This can be attributed to the additive inhibition effect of SLPI molecules and HSA particles. Since even loaded with SLPI, HSA nanoparticles still acquire a negative charge (i.e. negative zeta potential) and can electrostatically bind to NE molecules (**Figure 2.A**). This outcome is also interesting for the development of therapeutic anti-NE formulations for a wide

range of disease caused by overexpression of NE proteolytic activity especially in lungs (Korkmaz et al., 2010; Pandey et al., 2017).

### 3.5. Antibacterial activity assay

The antibacterial activities of free NE, free SLPI, NE-HSA-NPs, and SLPI-HSA-NPs were investigated *in vitro* against *P. aeruginosa* bacteria (**Figure 5**). As expected, both free NE and free SLPI exhibit an antibacterial activity (Belaouaj, 2002). Surprisingly, the bacterial growth in the presence of NE-HSA-NPs and SLPI HSA-NPs was markedly reduced when compared to that in the presence of free NE and SLPI, respectively. Moreover, in the presence of NE-HSA-NPs, the bacterial growth decreased significantly. Indeed, NE-HSA-NPs had an antibacterial effect 50 % further lower than that free NE against *P. aeruginosa*. This finding implies that encapsulated NE conserved its antibacterial activity. Various reports have shown that antibacterial activity of neutrophil serine proteases is enzymatic activity-dependent or independent. Regarding the latter statement, antibacterial amino acid sequences within the protease primary amino acid sequence have been suggested (Belaouaj, 2002). Accordingly, studies about the relative contribution of both antibacterial mechanisms (active NE versus denatured NE) are warranted.

*Figure 5: Bacterial growth of Pseudomonas aeruginosa H103 after overnight incubation at 37°C. H103) Control; NE) in the presence of free NE; NE-HSA-NPs) in the presence of NE-loaded HSA nanoparticles; SLPI) in the presence of free SLPI; and SLPIHSA-NE) in the presence of SLPI loaded HSA nanoparticles. Data from 6 different experiments were combined and represented as a percentage value relative to the control.*

Several positive points can be extracted from this work. Firstly, it shows a systematic study of HSA nanoparticles preparation via nanoprecipitation method. Secondly, it proved for the first time the reliability of using protein nanoparticles for the encapsulation of therapeutic proteins. Finally, the trustworthiness of using NE and SLPI as antibacterial agents in the time where alternative for antibiotic is of paramount importance. However, extended *in vitro* studies to better understand the loading and release behavior of the systems and *in-vivo* studies to prove the efficacy of these systems in biological environment are definitely required.

### 4. Conclusion

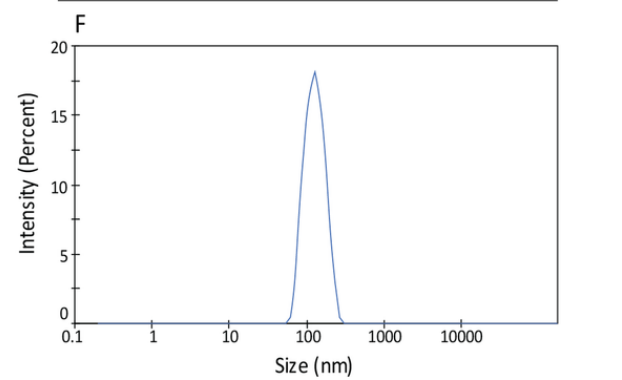
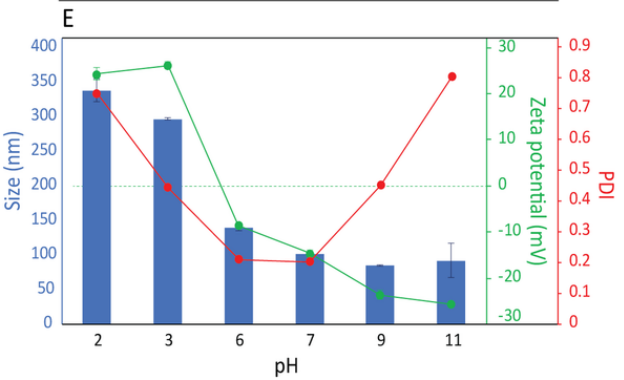
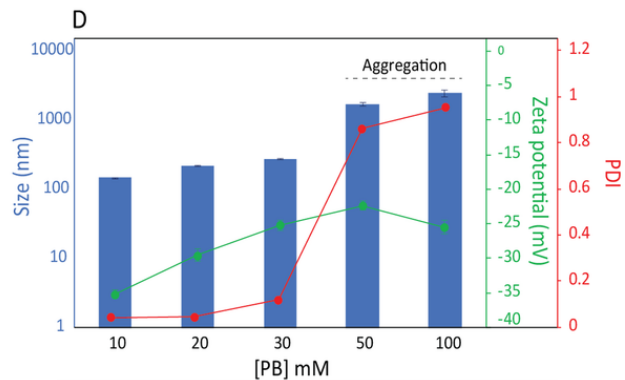
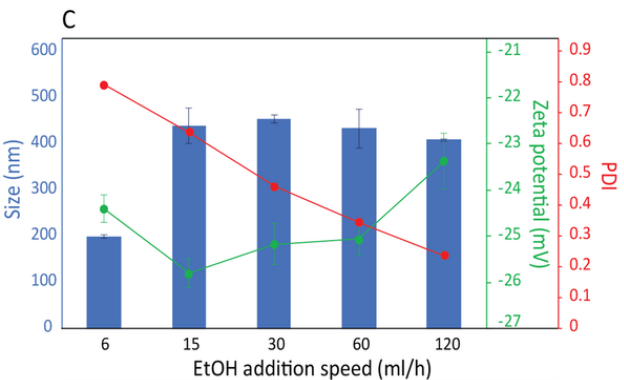
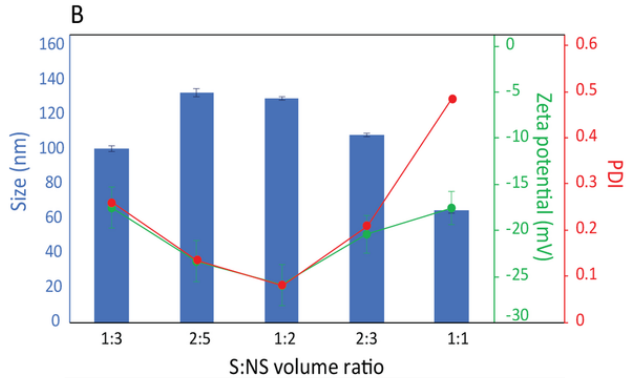
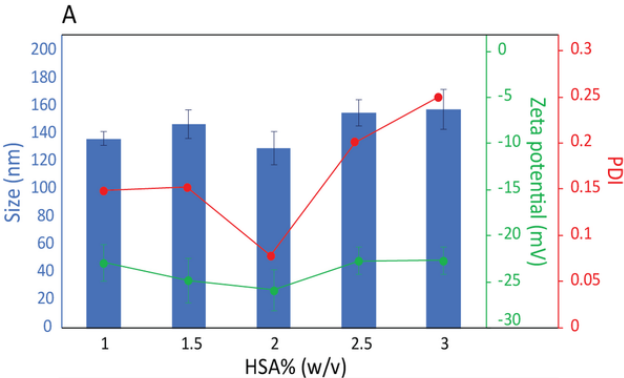
The development of albumin carrier for NE and SLPI was successfully achieved via nanoprecipitation-based process and the obtained dispersions were characterized in terms of size, size distribution and electrokinetic properties. From the optimization study, several parameters can be adjusted to obtain particles with desired colloidal properties according to the target applications and administration routes. In addition, gel electrophoresis and western blot studies indicate a successful encapsulation of both NE and SLPI within HSA protein matrix (under particulate form). The proteolytic activity of NE was lost *in vitro*, while its antibacterial activity was proved to be efficient. With respect to SLPI, it was shown that its encapsulation within HSA nanoparticles does not affect its antibacterial and its anti-NE activity. Both formulations, with warranted studies can prove their usefulness as antibacterial agents and as protective agents against tissue-degrading enzymes. Finally, to our knowledge, our work represents the first attempt of protein encapsulation within HSA nanoparticles. This attempt and according to the obtained results, the encapsulation of NE and SLPI in HAS based-nanoparticles can be considered as promising new route for personalized therapy.

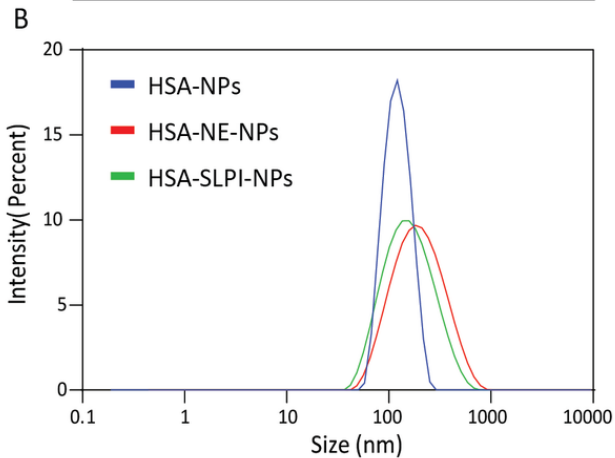
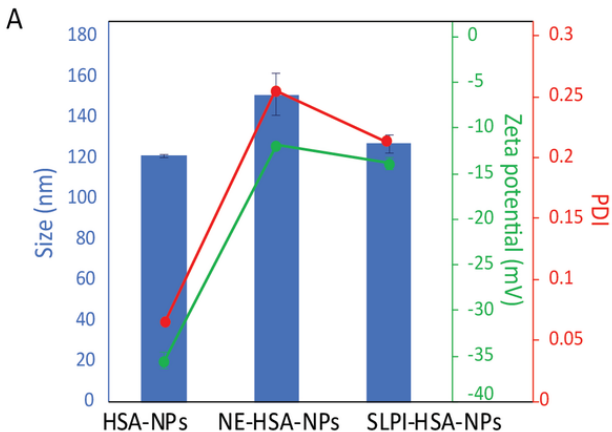
### References

Baici, A., 1990. Interaction of human leukocyte elastase with soluble and insoluble protein substrates. A practical kinetic approach. *Biochim. Biophys. Acta (BBA)/Protein Struct. Mol.* 1040, 355–364. [https://doi.org/10.1016/0167-4838\(90\)90133-Z](https://doi.org/10.1016/0167-4838(90)90133-Z)

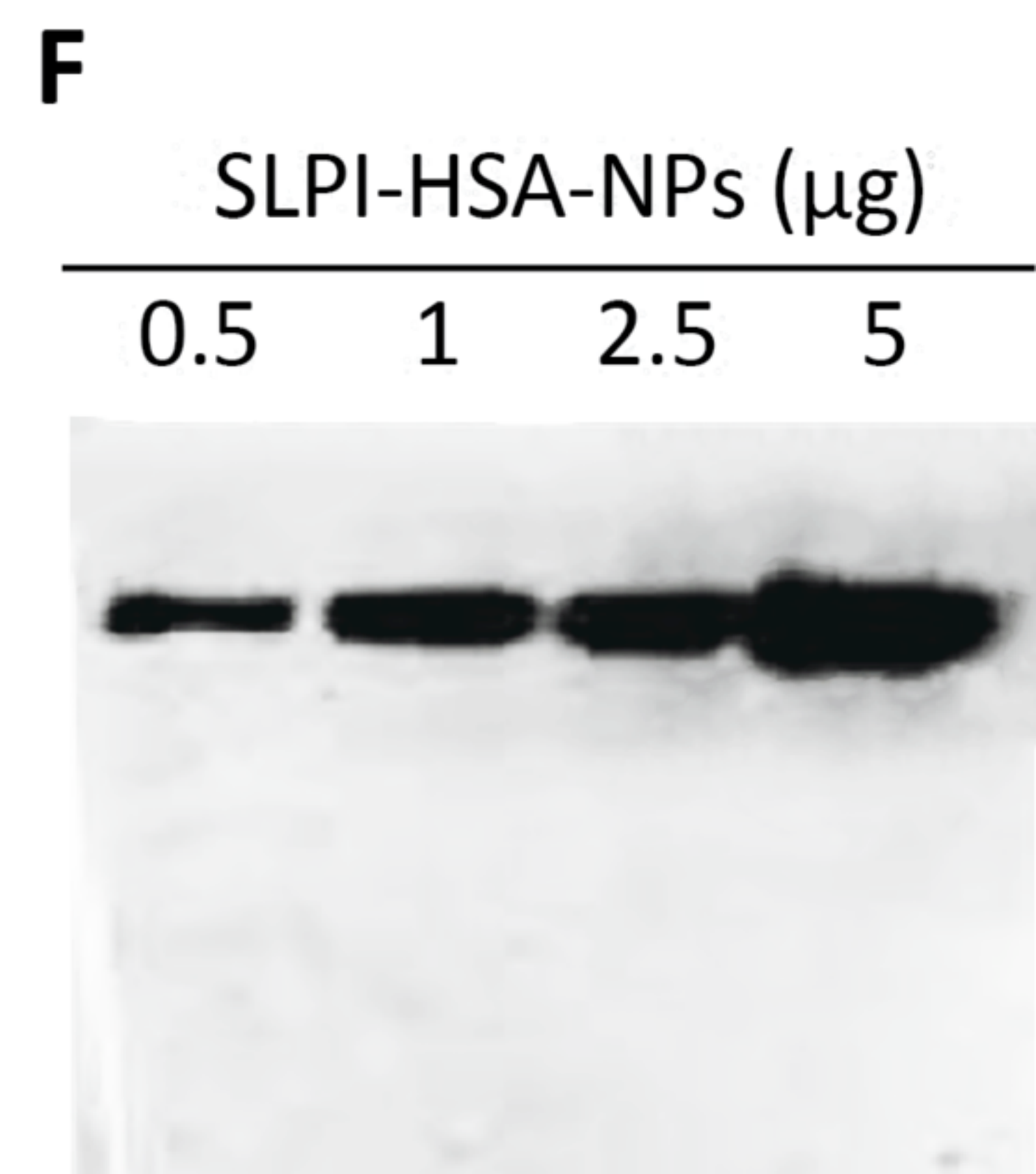
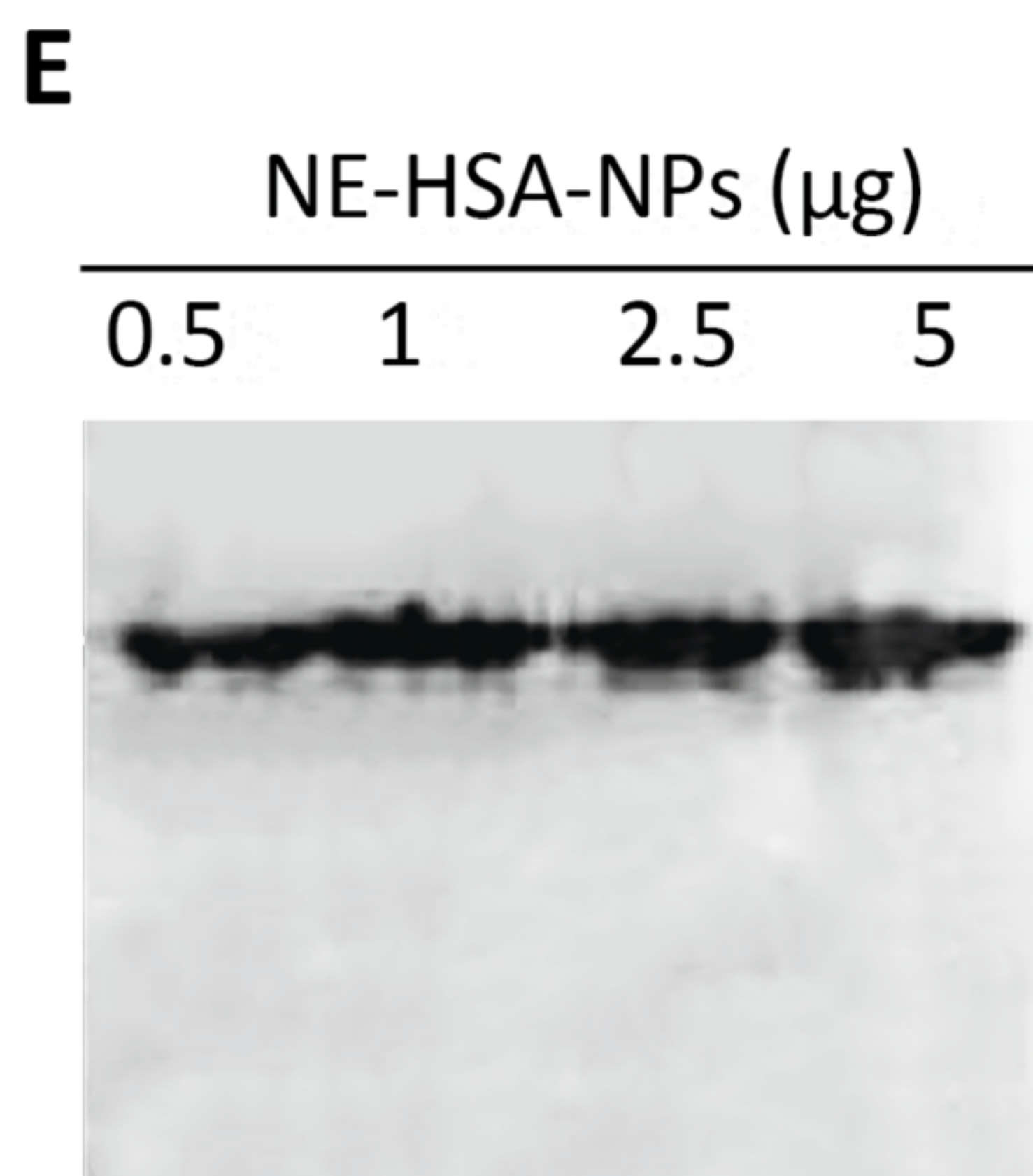
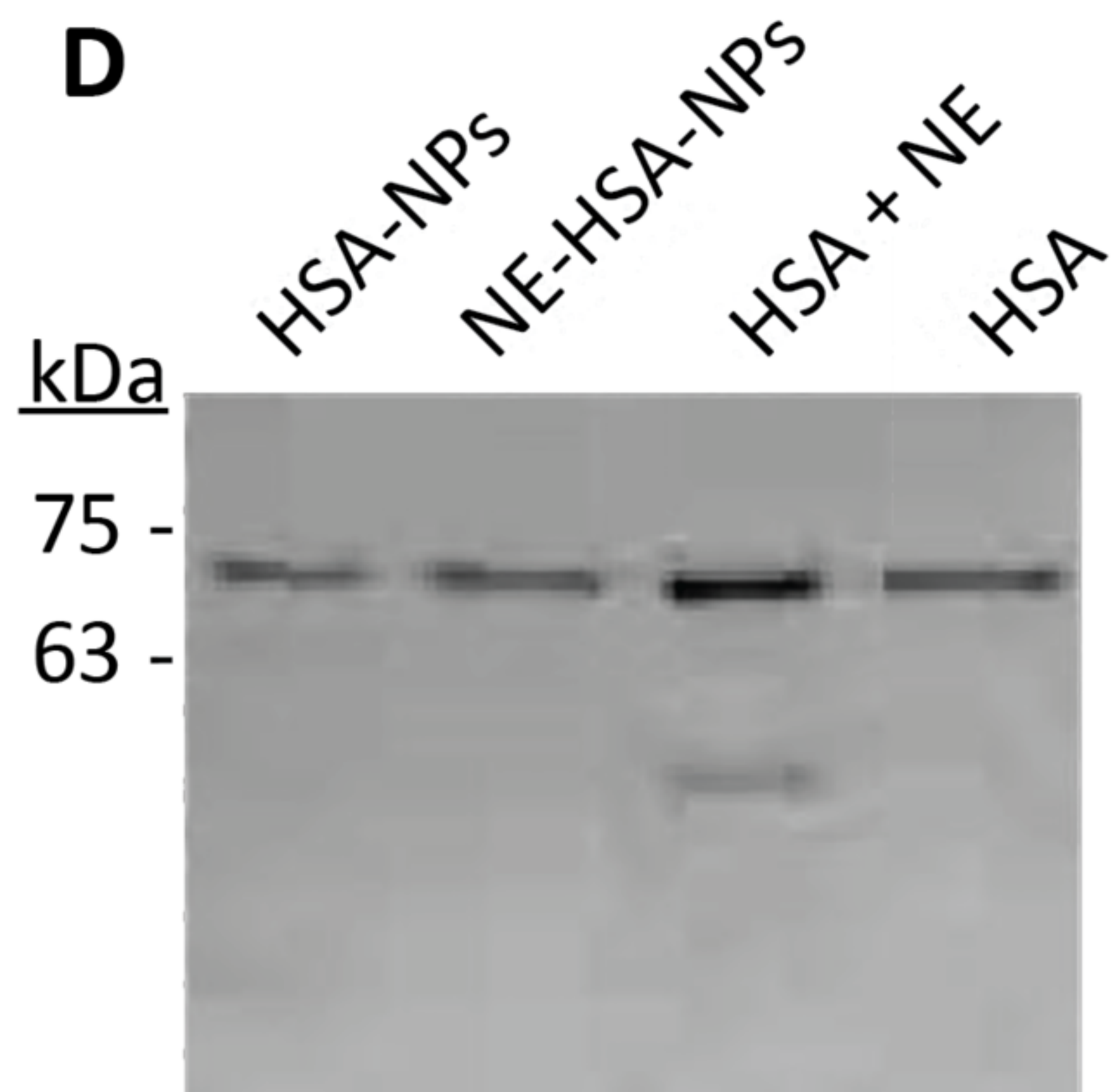
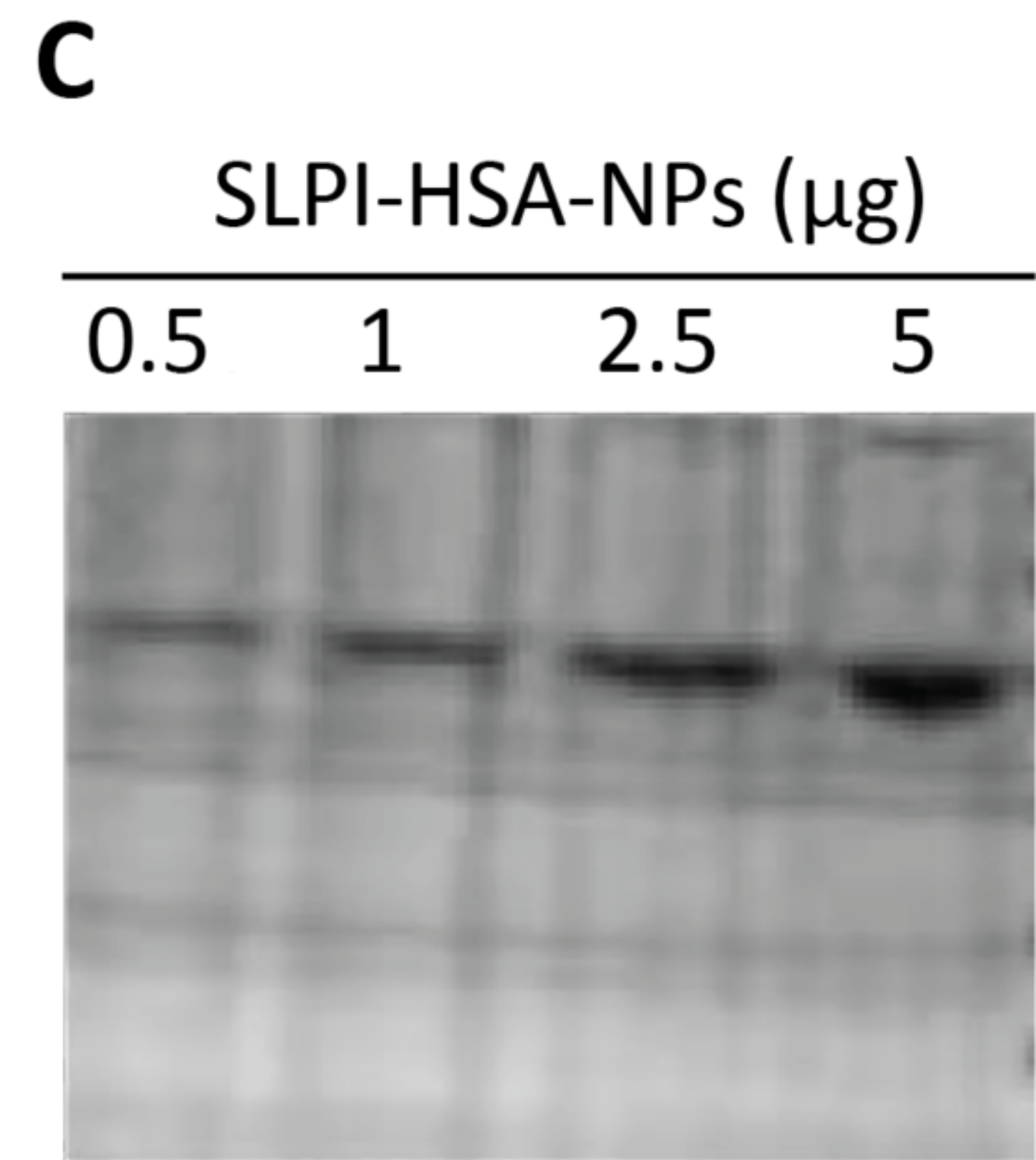
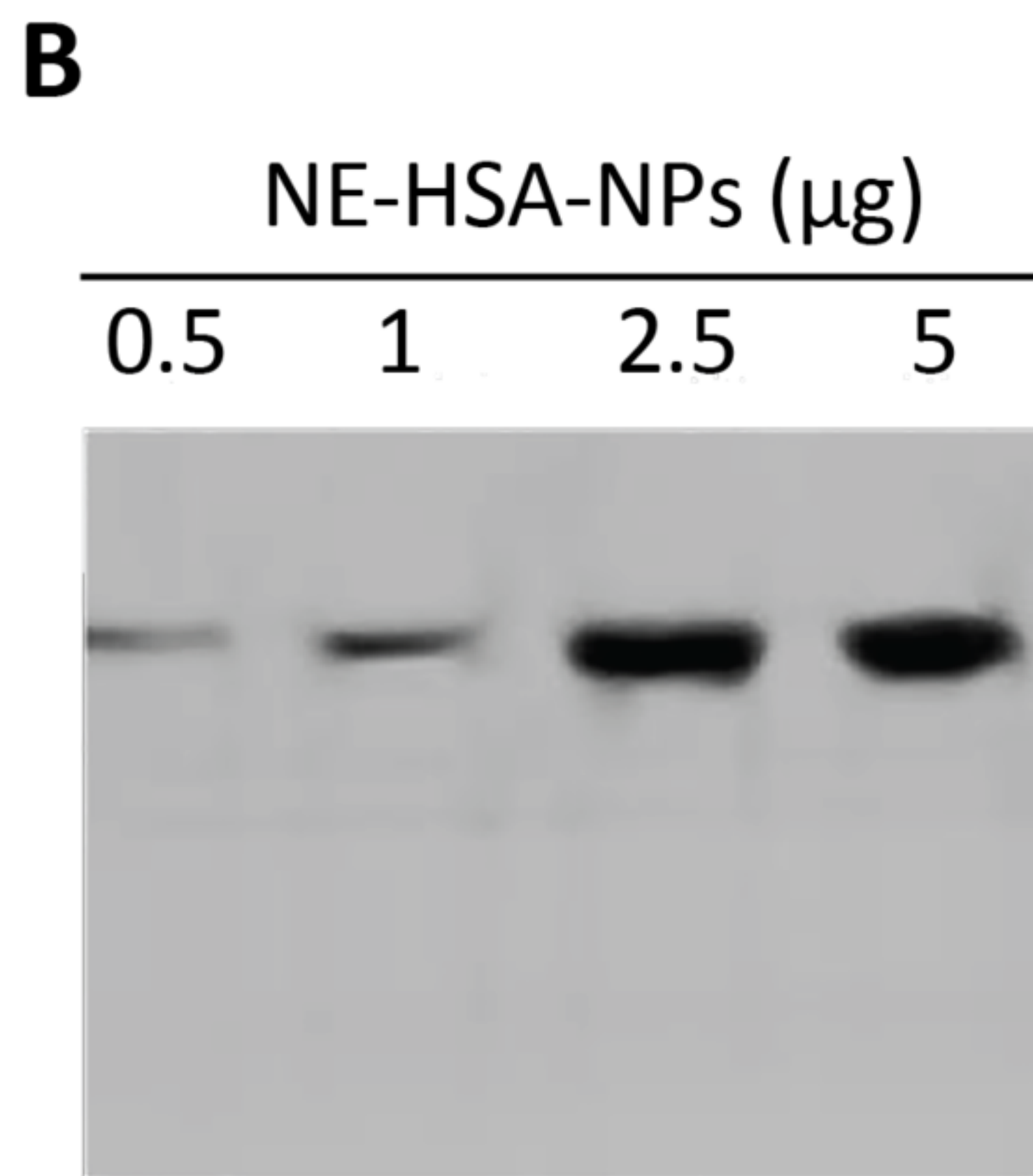
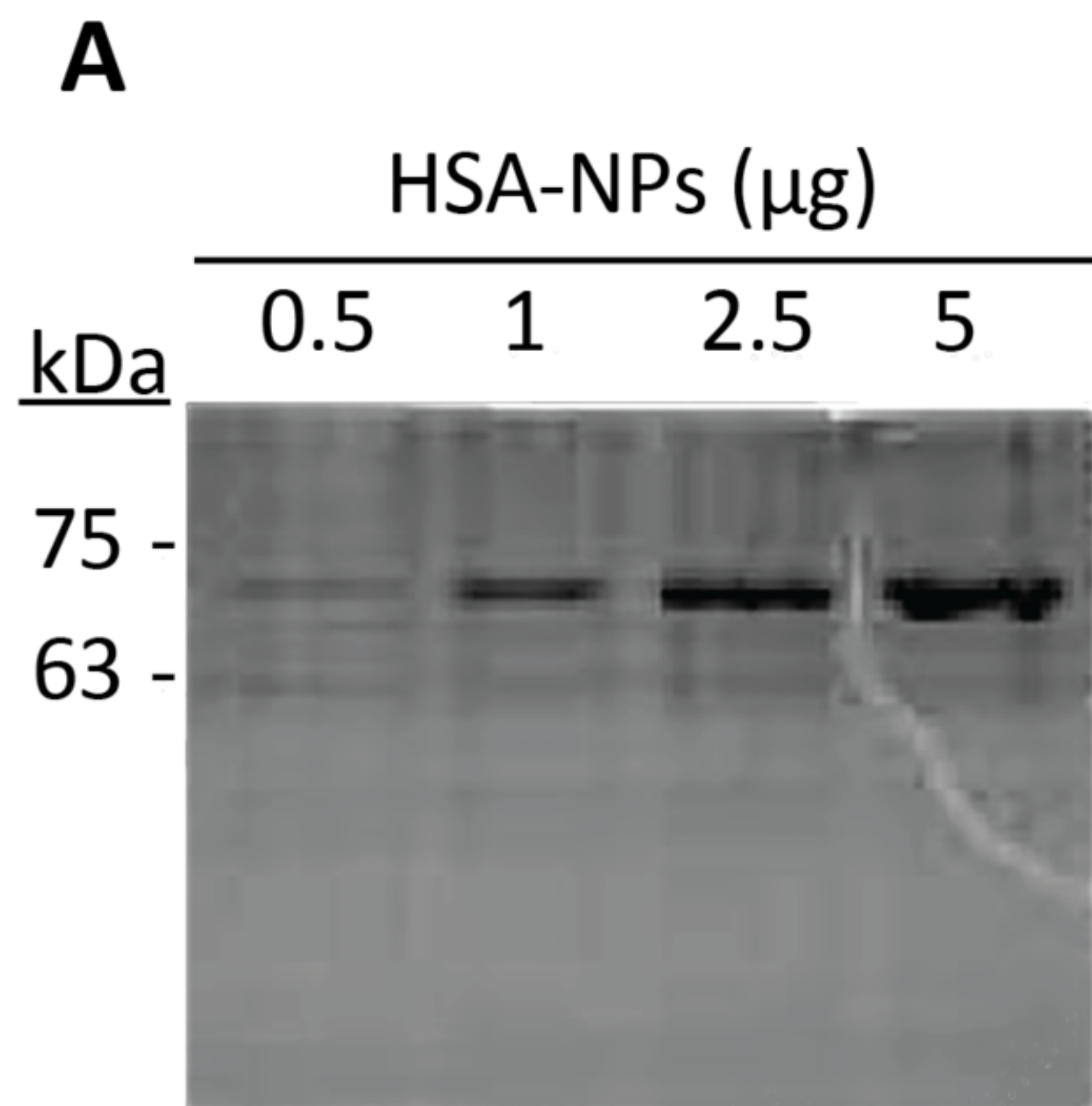
- Belaouaj, A., 2002. Neutrophil elastase-mediated killing of bacteria: Lessons from targeted mutagenesis. *Microbes Infect.* 4, 1259–1264. [https://doi.org/10.1016/S1286-4579\(02\)01654-4](https://doi.org/10.1016/S1286-4579(02)01654-4)
- Chaix, C., Pacard, E., Elaissari, A., Hilaire, J.-F., Pichot, C., 2003. Surface functionalization of oil-in-water nanoemulsion with a reactive copolymer: colloidal characterization and peptide immobilization. *Colloids Surfaces B Biointerfaces* 29, 39–52. [https://doi.org/10.1016/S0927-7765\(02\)00177-7](https://doi.org/10.1016/S0927-7765(02)00177-7)
- Danaei, M., Dehghankhold, M., Ataei, S., Hasanzadeh Davarani, F., Javanmard, R., Dokhani, A., Khorasani, S., Mozafari, M.R., 2018. Impact of particle size and polydispersity index on the clinical applications of lipidic nanocarrier systems. *Pharmaceutics* 10, 1–17. <https://doi.org/10.3390/pharmaceutics10020057>
- Davidov-Pardo, G., Joye, I.J., McClements, D.J., 2015. Food-Grade Protein-Based Nanoparticles and Microparticles for Bioactive Delivery, in: *Advances in Protein Chemistry and Structural Biology*. pp. 293–325. <https://doi.org/10.1016/bs.apcsb.2014.11.004>
- Edwards, J.V., Howley, P., Cohen, I.K., 2004. In vitro inhibition of human neutrophil elastase by oleic acid albumin formulations from derivatized cotton wound dressings. *Int. J. Pharm.* 284, 1–12. <https://doi.org/10.1016/j.ijpharm.2004.06.003>
- Elzoghby, A.O., Elgohary, M.M., Kamel, N.M., 2015. Implications of Protein- and Peptide-Based Nanoparticles as Potential Vehicles for Anticancer Drugs, in: *Protein and Peptide Nanoparticles for Drug Delivery*. Academic Press.; New York, pp. 169–221. <https://doi.org/10.1016/bs.apcsb.2014.12.002>
- Elzoghby, A.O., Samy, W.M., Elgindy, N. a., 2012. Protein-based nanocarriers as promising drug and gene delivery systems. *J. Control. Release* 161, 38–49. <https://doi.org/10.1016/j.jconrel.2012.04.036>
- Fessi, H., Puisieux, F., Devissaguet, J.P., Ammoury, N., Benita, S., 1989. Nanocapsule formation by interfacial polymer deposition following solvent displacement. *Int. J. Pharm.* 55, R1–R4. [https://doi.org/10.1016/0378-5173\(89\)90281-0](https://doi.org/10.1016/0378-5173(89)90281-0)
- Hanauer, M., Pierrat, S., Zins, I., Lotz, A., Sönnichsen, C., 2007. Separation of Nanoparticles by Gel Electrophoresis According to Size and Shape. *Nano Lett.* 7, 2881–2885. <https://doi.org/10.1021/nl071615y>
- Haro-Pérez, C., Quesada-Pérez, M., Callejas-Fernández, J., Casals, E., Estelrich, J., Hidalgo-Álvarez, R., 2003. Interplay between hydrodynamic and direct interactions using liposomes. *J. Chem. Phys.* 119, 628–634. <https://doi.org/10.1063/1.1578628>
- Hector, A., Kappler, M., Griese, M., 2010. In Vitro Inhibition of Neutrophil Elastase Activity by Inhaled Anti-Pseudomonas Antibiotics Used in Cystic Fibrosis Patients. *Mediators Inflamm.* 2010, 1–5. <https://doi.org/10.1155/2010/809591>
- Herrera Estrada, L.P., Champion, J.A., 2015. Protein nanoparticles for therapeutic protein delivery. *Biomater. Sci.* 3, 787–799. <https://doi.org/10.1039/C5BM00052A>
- Joye, I.J., McClements, D.J., 2013. Production of nanoparticles by anti-solvent precipitation for use in food systems. *Trends Food Sci. Technol.* 34, 109–123. <https://doi.org/10.1016/j.tifs.2013.10.002>
- Korkmaz, B., Horwitz, M., Jenne, D., Gauthier, F., 2010. Neutrophil elastase, proteinase 3, and cathepsin G as therapeutic targets in human diseases. *Pharmacol. Rev.* 62, 726–759. <https://doi.org/10.1124/pr.110.002733.726>

- Kratz, F., 2008. Albumin as a drug carrier: Design of prodrugs, drug conjugates and nanoparticles. *J. Control. Release* 132, 171–183. <https://doi.org/10.1016/j.jconrel.2008.05.010>
- Langer, K., Balthasar, S., Vogel, V., Dinauer, N., Von Briesen, H., Schubert, D., 2003. Optimization of the preparation process for human serum albumin (HSA) nanoparticles. *Int. J. Pharm.* 257, 169–180. [https://doi.org/10.1016/S0378-5173\(03\)00134-0](https://doi.org/10.1016/S0378-5173(03)00134-0)
- Lerman, I., Hammes, S.R., 2018. Neutrophil elastase in the tumor microenvironment. *Steroids* 133, 96–101. <https://doi.org/10.1016/j.steroids.2017.11.006>
- Majchrzak-Gorecka, M., Majewski, P., Grygier, B., Murzyn, K., Cichy, J., 2016. Secretory leukocyte protease inhibitor (SLPI), a multifunctional protein in the host defense response. *Cytokine Growth Factor Rev.* 28, 79–93. <https://doi.org/10.1016/j.cytogfr.2015.12.001>
- Miller, K.W., Evans, R.J., Eisenberg, S.P., Thompson, R.C., 1989. Secretory Leukocyte Protease Inhibitor Binding to mRNA and DNA as a Possible Cause of Toxicity to *Escherichia coli*. *J. Bacteriol.* 171, 2166–2172. <https://doi.org/10.1128/jb.171.4.2166-2172.1989>
- Pandey, K.C., De, S., Mishra, P.K., 2017. Role of Proteases in Chronic Obstructive Pulmonary Disease. *Front. Pharmacol.* 8, 512. <https://doi.org/10.3389/fphar.2017.00512>
- Rahimnejad, M., Jahanshahi, M., Najafpour, G.D., 2006. Production of biological nanoparticles from bovine serum albumin for drug delivery. *J. Biotechnol.* 5, 1918–1923. <https://doi.org/10.4314/ajb.v5i20.55912>
- Rhaese, S., Von Briesen, H., Rüksamen-Waigmann, H., Kreuter, J., Langer, K., 2003. Human serum albumin-polyethylenimine nanoparticles for gene delivery. *J. Control. Release* 92, 199–208. [https://doi.org/10.1016/S0168-3659\(03\)00302-X](https://doi.org/10.1016/S0168-3659(03)00302-X)
- Tarhini, M., Greige-Gerges, H., Elaissari, A., 2017. Protein-based nanoparticles: From preparation to encapsulation of active molecules. *Int. J. Pharm.* 522, 172–197. <https://doi.org/10.1016/j.ijpharm.2017.01.067>
- Tsai, Y.-F., Hwang, T.-L., 2015. Neutrophil elastase inhibitors: a patent review and potential applications for inflammatory lung diseases (2010 – 2014). *Expert Opin. Ther. Pat.* 25, 1145–1158. <https://doi.org/10.1517/13543776.2015.1061998>
- Zhao, D., Zhao, X., Zu, Y., Li, J., Zhang, Y., Jiang, R., Zhang, Z., 2010. Preparation, characterization, and in vitro targeted delivery of folate-decorated paclitaxel-loaded bovine serum albumin nanoparticles. *Int. J. Nanomedicine* 5, 669–77. <https://doi.org/10.2147/IJN.S12918>

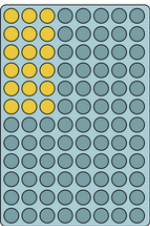








A

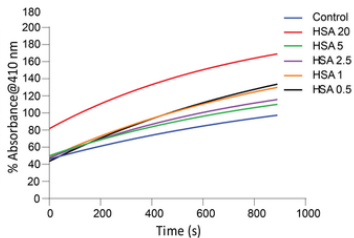


**Control**

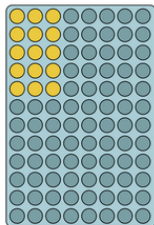
- 85  $\mu$ l activity buffer
- 10  $\mu$ l NE
- 5  $\mu$ l DMSO
- 50  $\mu$ l substrat

**Samples**

- 85  $\mu$ l activity buffer
- 10  $\mu$ l NE
- 5  $\mu$ l HSA (20, 5, 2.5, 1, 0.5  $\mu$ g)
- 50  $\mu$ l substrat



B

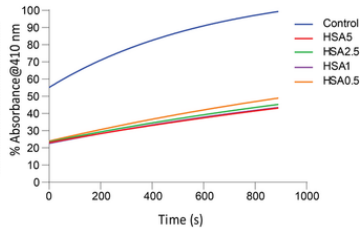


**Control**

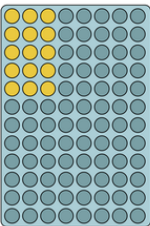
- 85  $\mu$ l activity buffer
- 10  $\mu$ l NE
- 5  $\mu$ l DMSO
- 50  $\mu$ l substrat

**Samples**

- 85  $\mu$ l activity buffer
- 10  $\mu$ l NE
- 5  $\mu$ l HSA-NPs (5, 2.5, 1, 0.5  $\mu$ g)
- 50  $\mu$ l substrat



C

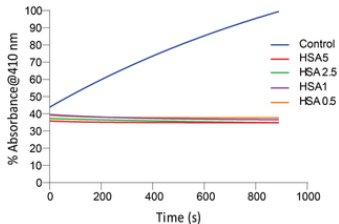


**Control**

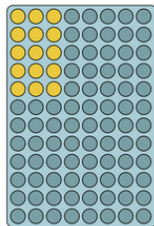
- 85  $\mu$ l activity buffer
- 10  $\mu$ l NE
- 5  $\mu$ l DMSO
- 50  $\mu$ l substrat

**Samples**

- 95  $\mu$ l activity buffer
- 5  $\mu$ l NE-HSA-NPs (5, 2.5, 1, 0.5  $\mu$ g)
- 50  $\mu$ l substrat



D

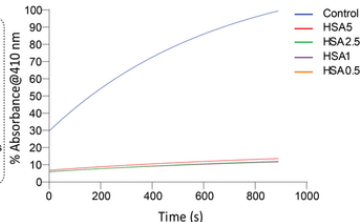


**Control**

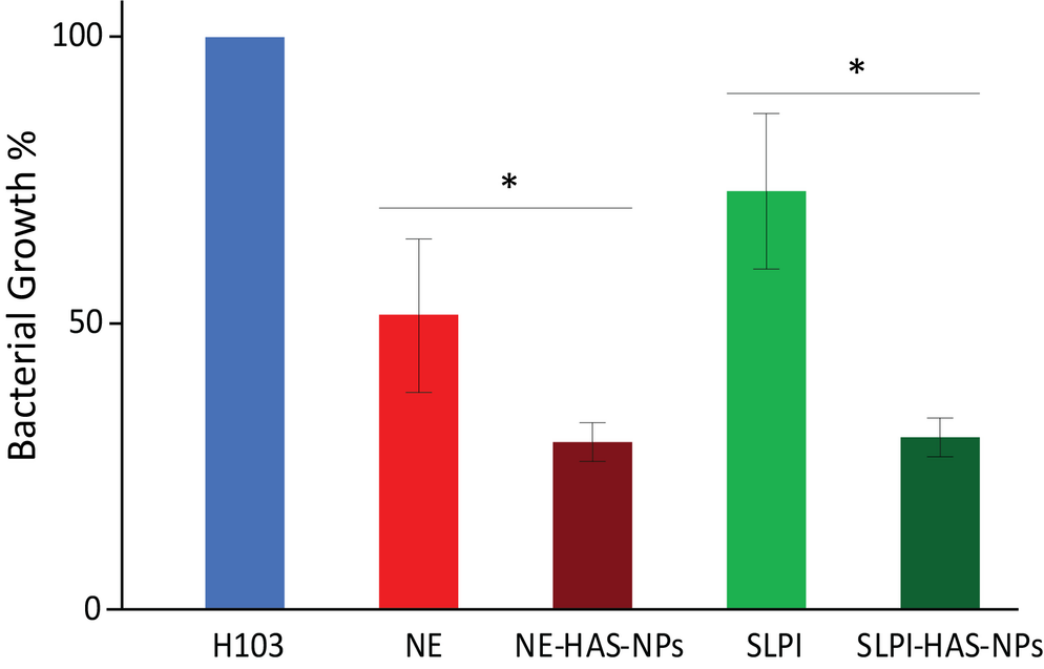
- 85  $\mu$ l activity buffer
- 10  $\mu$ l NE
- 5  $\mu$ l DMSO
- 50  $\mu$ l substrat

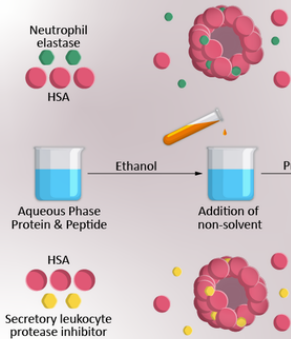
**Samples**

- 85  $\mu$ l activity buffer
- 10  $\mu$ l NE
- 5  $\mu$ l SLPI-HSA-NPs (5, 2.5, 1, 0.5  $\mu$ g)
- 50  $\mu$ l substrat









Nanoparticle preparation

Elastase loaded  
HSA nanoparticles



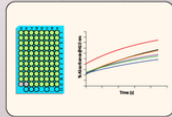
SLPI loaded  
HSA nanoparticles



Characterization



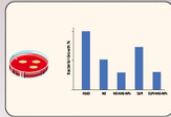
Enzymatic assays



Gel electrophoresis & western blot



Antibacterial activity assays



Nanoparticle evaluation